12º Congresso Brasileiro de Engenharia de Fabricação
10 a 12 de maio de 2023, Brasília, DF, Brasil

EFFECT OF LASER POWER AND POWDER MORPHOLOGY ON SURFACE ROUGHNESS OF TI6AL4V PRODUCED BY LASER POWDER - DIRECTED ENERGY DEPOSITION

Geovana Eloizi Ribeiro
Vincent Edward Wong Diaz
Willian Roberto Valicelli Sanitá
Alessandro Roger Rodrigues
Mechanical Engineering Department, São Carlos School of Engineering, University of São Paulo
e-mails: vwong.ufs@gmail.com, geovana_rib@usp.br, willian.r.sanita@usp.br, roger@sc.usp.br,
Reginaldo Teixeira Coelho
Production Engineering Department, São Carlos School of Engineering, University of São Paulo
rtcoelho@sc.usp.br

Abstract: Additive manufacturing of metals has emerged as a technology capable of producing complex metal parts in the "near net shape" format, performing repairs, and creating components with gradient material, enabling manufacturing parts with high added value and low production. Directed Energy Deposition from Laser and Powder (LP-DED) is one of the categories of the additive manufacturing process by which concentrated thermal energy allows the metallic powder to melt. These applications have been attractive to different areas such as aerospace, automotive, and medical. In the medical field, its application has focused on creating implants, prostheses, instruments, and medical devices. Ti6Al4V titanium alloys have stood out due to their high mechanical strength, high corrosion resistance, low density, and good biocompatibility. One of the literature challenges reflects the roughness given to printed parts by the LP-DED process, which can affect the osseointegration of prostheses and implants, linked to their recovery time and success. This article evaluates the roughness of Ti6Al4V parts obtained from the LP-DED process using two types of powder. The first is produced by gas atomization, and the second by advanced plasma atomization. Subsequently, eight specimens were fabricated by LP-DED on pure Ti substrate. The laser power was another input variable ranging from 300 W to 345 W with a 15 W increment. Samples were cleaned with deionized water and acetone using ultrasonic vibration. Then, we evaluated the roughness of the samples using a confocal microscope. The Powder morphology of the powder used showed that powder produced by gas atomization presented a distribution non-gaussian, with flakes, pores, and satellites. The powder made by advanced plasma atomization showed a gaussian distribution, with fewer pores quantity and less presence of satellites and flakes when compared with gas atomization powder.

Keywords: *Directed Energy Deposition; Roughness; Ti6Al4V, Additive Manufacturing.*

1. INTRODUCTION

Titanium alloy is a material that possesses high specific strength, moderate Young's Modulus, and excellent corrosion resistance; these attributes have been used in areas such as aerospace, marine, chemical, military, and biomedical (Yang *et al*., 2022). In biomedical applications, titanium alloy is broadly used in implants and prostheses. These devices spend most of their cycle of life inside the human body. For this reason, titanium alloy needs to satisfy some requirements related to compatibility (Mechanical, Chemical, and Biological) between the user and the material. When the device's compatibility is improved, it also enhances the function of the implant, which works similarly to the original tissue. It reduces the risk of suffering widely known diseases that are mostly associated with poor functionality of the implant. Ti6Al4V alloy is an α+β alloy, considered a first-generation alloy most used. The Al is added to stabilize the α phase, which increases the β transformation temperature, while V stabilizes the β phase and reduces it.

Additive Manufacturing (AM) is a set of techniques that enable the creation of metallic parts with an agreed value high and a low production level. This technique is based on adding material layer upon layer, contrary to subtractive manufacturing (Sivamani *et al.*, 2020). It has been used in many materials, including metallics polymerics, ceramics, and composites (Gibson *et al.*, 2021). Metal additive Manufacturing (MAM) can be classified initially into two groups Powder Bed Fusion (PBF) and Directed Energy Deposition (DED). In DED, the type of material can be powder and wire, and the heat source can be from Laser, Plasma Arc, and Electron Beam melting. Specifically, Laser Powder Directed Energy Deposition (LP-DED) uses the incidence of a high-power laser on metallic powder, coaxially delivered, forming a melt pool that solidifies on a substrate.

Although MAM has numerous advantages, surface finishing of fabricated parts remains one of the major concerns (Leary, 2017). In biocompatibility terms, the surface roughness plays a role important in guaranteeing osseointegration

(Jemat *et al.*, 2015); recently, studies have shown the influence of the process parameters such as deposition strategy, process parameters, layer thickness, laser power, and scanning speed in the part roughness (Oyelola *et al*., 2018; Azarniya *et al*., 2019; Kwak *et al*., 2021). However, the results observed in the literature using LP-DED showed a different range of surface roughness due to the powder's quality, including (morphology, particle size), machine configuration, the necessity of a controlled atmosphere, and adjusting the process parameters.

In roughness terms, the surfaces generated by the LP-DED method are characterized by rough aspects (Selcuk, 2011). In the biomedical area, there is research pointing out that implant fixation is a product of surface roughness and bone position (Wong *et al*., 1995). In shear cases, surfaces with higher roughness offer greater bonding with bone tissue, providing greater resistance to ruptures (Hacking *et al*., 2012).

According to Ye *et al*. (2021), surface finishing plays an important role in the fatigue performance of the part. Generally, the parts produced by MAM need to present a better surface finish in as-built conditions (Bagehorn *et al*., 2017; Gockel *et al*., 2019). It is due to three reasons: 1) the adherence of powder semi-melted in the part's surface. This phenomenon is called balling and results from regrouping powder particles under inhomogeneous heating conditions (Tolochko *et al*., 2004); 2) The staircase phenomenon. It allows visualizing the layer mark caused by the offset in part with an inclined or curved surface (Li *et al*., 2016); 3) and the appearance of pores or regions with melting incomplete. Greitemeier *et al*. (2016) highlighted that although the mechanical properties, microstructure, and other factors affect the fatigue performance in parts produced by MAM, surface finishing is the main cause of poor fatigue performance compared with milled parts.

Chan *et al*. (2013) analyzed the fatigue life of titanium alloys manufactured by Electron Beam Melting and Laser Beam Melting. They established a double logarithm plot of various Ti6Al4V samples that allow the correlation of the maximum surface roughness (Ra) with the mean fatigue life cycle. Also, the Laser Beam melting samples obtained a longer life than Electron Beam Melting.

Various roughness ranges are suitable for biomedical implants; the values vary according to the raw material, type of manufacturing, desired application, and post-processing. According to Svetlizky *et al*. (2007), good dental implants should have Ra between 0.5 and 1.0 μm, and it is important to consider that the removal torque increases when growing Ra up to a certain value. Wennerberg and Albrektsson (2000) found commercial Sa roughness ranging from 0.54 to 2.09 μm. However, larger Ra roughness intervals between 45 and 53.25 μm showed a high cell proliferation and adhesion capacity in Titanium (Zareidoost *et al*., 2012). In addition, according to Hatamleh *et al*. (2018), Sq roughness from 2.81 to 16.68 μm indicated equal biocompatibility when considering different surface treatments in Ti6Al4V implants such as polishing, sandblasting, acid etching, and electrochemical treatment. Finally, Krishna *et al*. (2010) declare that bone tissue can adapt to surface irregularities with 1 to 100 μm height and that changing the surface topography of an implant can greatly improve its stability.

This paper aims to establish the relationship between part roughness, powder morphology, and laser power when printing Ti6Al4V by LP-DED and compare these results to those found in the literature, indicating some possible applications.

2. MATERIALS AND METHODS

The LP-DED machine BeAM Modulo 250 and Ti6Al4V powder (grade 23) manufactured by Carpenter Additive and Ti6Al4V powder (grade 5) manufactured by AP&C were applied in this study. The chemical composition of each powder is described in Tab. 1. The Argon was used as a carrier, central, and shield work gas. The scanning speed of 2000 mm/min and the powder feed rate of 5.4 g/min were kept constant. The material used as a subtract was composed of pure titanium close to the deposition area of the cubes. The dimensions of the specimens fabricated were 15 mm in length, 15 mm in width, and 6 mm in height. The process parameters of each specimen are described in Tab. 2.

Table 1. Chemical composition of both study powders, including the variation of O and N as an interstitial element

	Al	C	H	Fe	N	O	Ti	V	Y
Carpenter	5.5 - 6.5	0 - 0.8	0 - 0.01	0 -0.25	0 - 0.03	0 - 0.13	balance	3.5 - 4.5	0 - 0.05
AP&C	5.5 - 6.75	0 - 0.8	0 - 0.01	0 - 0.4	0 - 0.05	0 - 0.2	balance	3.5 - 4.5	-

Table 2. Process Parameters used with laser power between 300 W to 345 W

Specimen #	Laser Power (W)	Powder manufacturer	Specimen #	Laser Power (W)	Powder manufacturer
1	300	Carpenter	5	300	AP&C
2	315		6	315	
3	330		7	330	
4	345		8	345	

Before measuring the roughness, the samples were cleaned with acetone and deionized water under ultrasonic vibration at 35 kHz by employing a sonicator machine, Julabo USR 1, to remove the powder particles that adhered to the study surface. Besides average center roughness (Sa) typically utilized for biomedical applications, this research also measured the peak-valley mean roughness (Sz), skewness (Ssk), and kurtosis (Sku) roughness by using a microscope confocal Olympus OLS4100.

3. Results and discussions

3.1. Powder characterization

As mentioned above, two powders were used in this study. The first powder was a Carpenter Ti6Al4V ELI grade 23 alloy produced by gas atomization and shown in Fig. 1a. The particle size ranges from 45 - 106 µm. The results of the particle size distribution of the powders are shown in Fig. 1b, which was measured by the optical microscope Olympus OLS4100. This powder has mostly spherical morphology with the presence of satellites, pores, and flakes to a lesser extent.

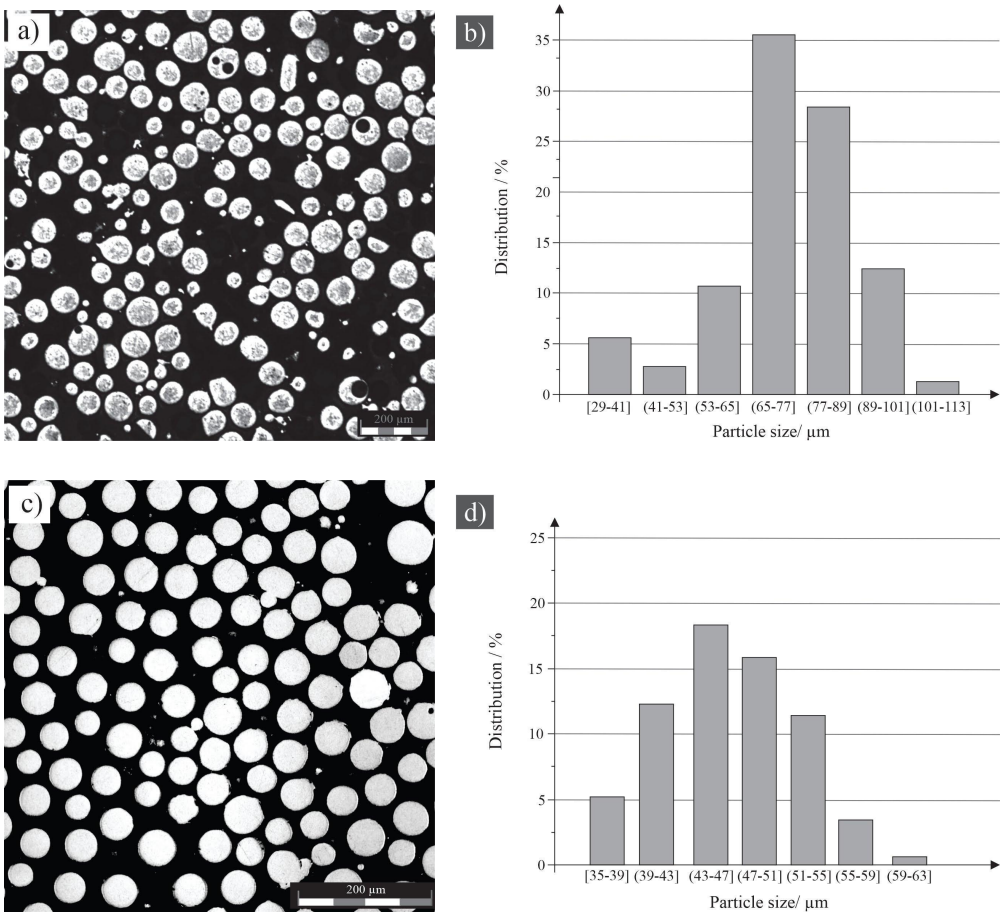

Figure. 1. Optical microscopy powder a) Carpenter with the presence of satellite, pores, and flakes to a lesser extent. b) Particle size distribution Ti6Al4V Carpenter powder with behavior non-gaussian. c) AP&C with particle size close to the mean. d) Particle size distribution Ti6Al4V AP&C powder with behavior close to the Gaussian distribution.

The second Powder, Ti6Al4V grade 5 alloy produced by advanced plasma atomization (APA™) and shown in Fig. 1c, was provided by AP&C. The particle size ranges from 45- 90 µm. This powder has mostly spherical morphology, with less presence of flakes and satellites when compared with Carpenter powder and particle size close to the mean. The results of the particle size distribution of the powders are shown in Fig. 1d.

The main difference between both types of powder is the reduction of the content of interstitial elements such as N or O. This difference plays a key role in microstructures because they are strong α-stabilizers and influence the α-to-β transition temperature. Low interstitial element content improves ductility and fracture toughness (Antonysamy, 2012). In Ti6Al4V, Grade 23, the reduction of oxygen content is limited to 0.13% (maximum). In Ti64Al4V grade 5, the reduction of oxygen content is restricted to 0.2% (max).

3.2. Process Parameters

In this study, the powder feed rate and laser powder were essential to construct cubes with uniform geometry. The powder feed rate was obtained by capturing and measuring the powder mass for one minute using a horizontal disk powder feeder. To Carpenter powder, the rotation of the horizontal feed disk was defined in values of 1, 1.4, and 2 rpm. To AP&C powder, the rotation was determined at 1, 1.4, and 1.6 rpm. This procedure was performed three times for each rotation to ensure measurement reliability.

In Figure 2, it is possible to observe that the precision of the powder feed rate is more efficient when the particle size has a behavior similar to the Gaussian distribution. When combined with the laser power, the powder particle size and the powder feed rate directly affect the porosity and tiny void generation in LP-DED, as Averardi *et al*. (2020) described. In terms of laser power, all the samples showed a good grip, without burns, and with a linear deposition. At the beginning of the deposition process, the melt pool was composed predominantly of powder, creating a small lack of fusion at the beginning of the layers. Using the subtract near the deposition area allowed the creation of density energy focused, favoring the fusion in subsequent layers, creating a good underlayer adhesion of the laser spot at the beginning and the final of the deposition trajectory.

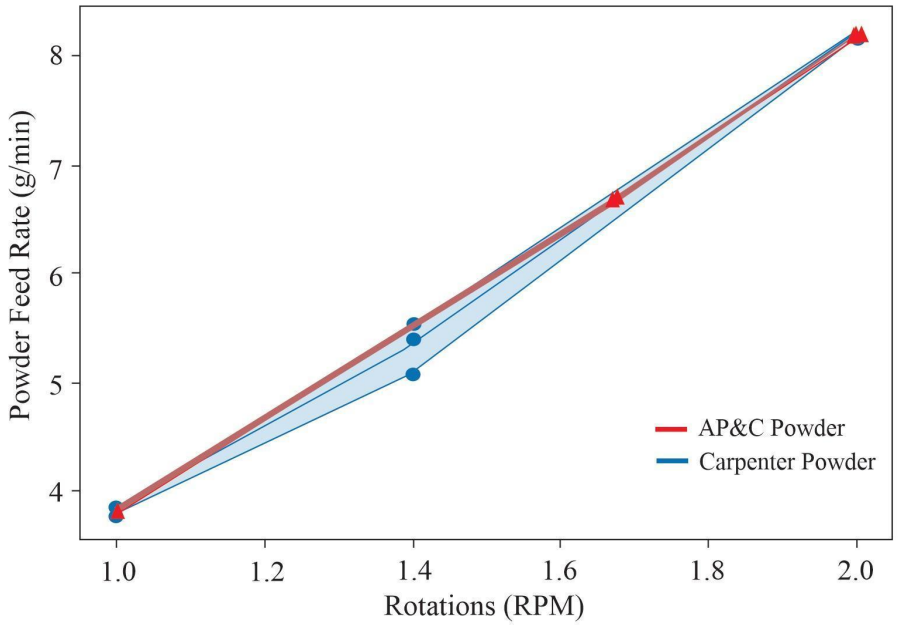

Figure 2. Rotation (rpm) vs. powder feed rate to both powders.

From the viewpoint of geometrical features, the dimensions obtained of parts were 15.73 x 15.77 x 6.04. the geometrical features of one sample are shown in Figure 3. The values in X and Y superior of 15 mm are associated with the spot diameter of the laser. When the deposition occurs, the origin of the coordinate does not consider the middle of the circumference of the laser spot at the beginning and the final of the deposition trajectory.

3.3. Roughness Evaluation

The finishing data revealed a tendency in both averages (Sa) and quadratic (Sq) roughness parameters to decrease when increasing the laser power, as seen in Fig. 4. The powder is more densely melted since the degree of fusion increases with laser power. Furthermore, comparing the two powders of different manufacturers, the AP&C powder showed roughness ranges with higher values relative to the Carpenter one.

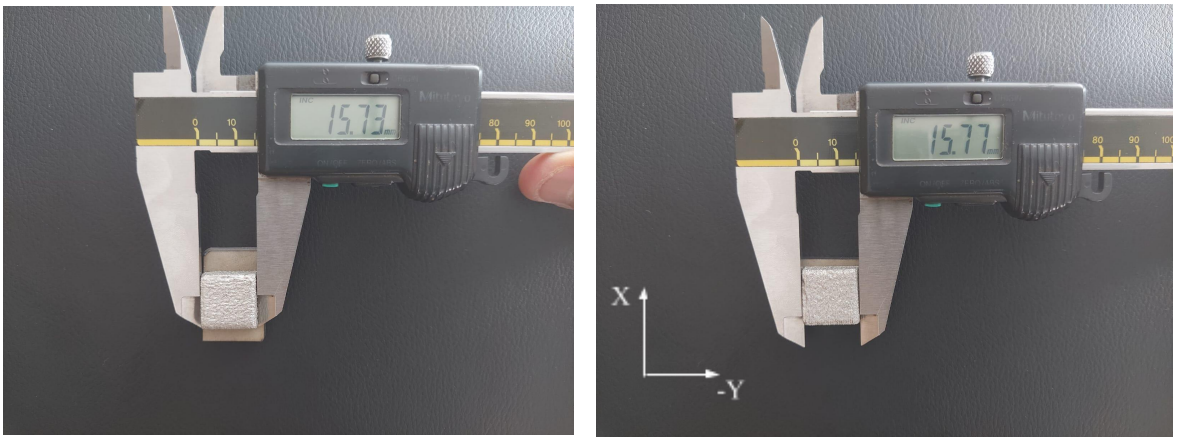

Figure. 3. Geometrical features of one sample show a measure superior to the initial geometry.

These Sa roughness findings are slightly lower than those of Zareidoost *et al*. (2012), while Sq ones are higher than those of Hatamleh *et al*. (2018). Such differences result from the as-built condition of the samples studied in this paper and the post-processing or surface treatment carried out in specimens from the literature. A way to reach the desired roughness ranges, such as those obtained by Wennerberg and Albrektsson (2000), is to change the process parameters once the Sa and Sq roughness decrease as the laser power increases, allowing receiving surfaces with better finishing and less need for post-processing.

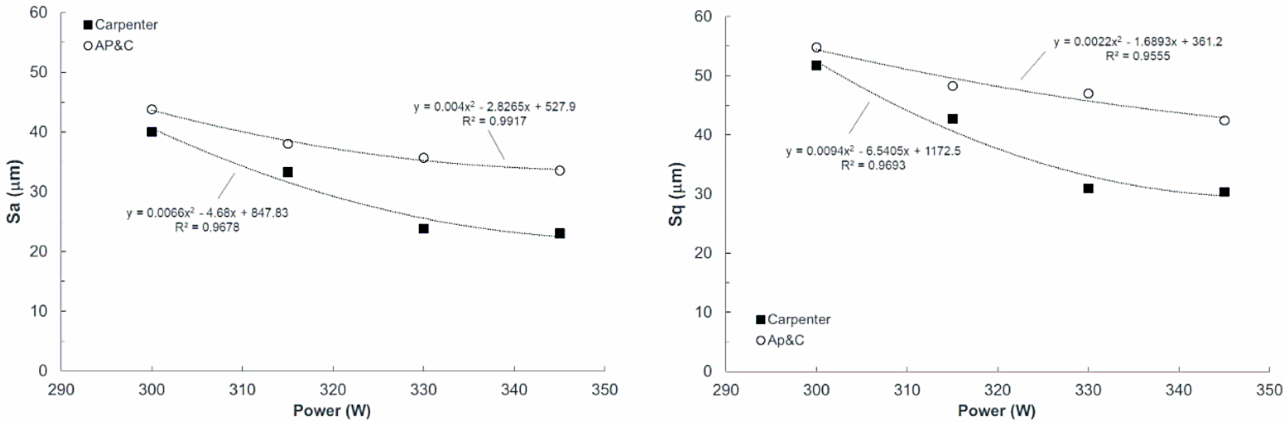

Figure 4. Sa and Sq roughness as a function of laser power and Ti powder provider.

Examining the statistical parameters skewness and kurtosis from Fig. 5, it is noticed that Ssk values are positive regardless of the laser power and powder provider, which means that the surface produced by LP-DED presents material concentration on valleys. Negative levels would indicate a plateau-based surface or flat peaks. Although the skewness analysis can be ternary (negative, zero, or positive), two minimum points for each powder manufacturer are identified in 321 W and 340 W, respectively, for Carpenter and AP&C providers. This finding can be particularly useful since very high positive skewness magnitudes were measured by showing a surface highly skewed with a greater absence of material on the sample surface.

When evaluating the kurtosis, it is verified that all values are greater than three, which means that the printed surface presents large peaks or valleys (spiky surface). This surface texture produced by LP-DED can be interesting when applied to implants, i.e., a spiky topography (Sku > 0) with a predominance of peaks (Ssk > 0) could work as cells housing, maximize their attachment at microscope level, and consequently, the formation of bone matrix around the implant.

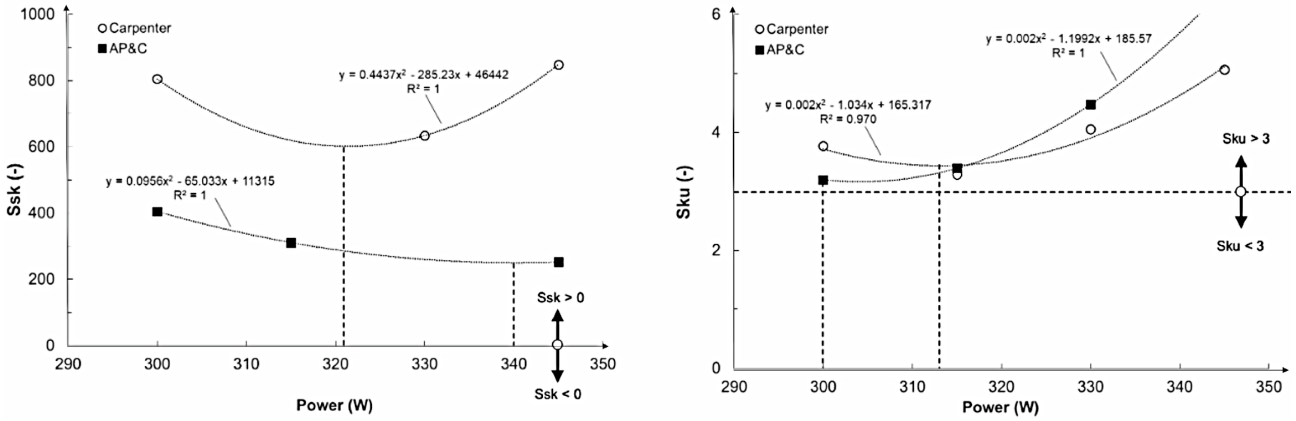

Figure 5. Ssk and Sku roughness as a function of laser power and Ti powder provider.

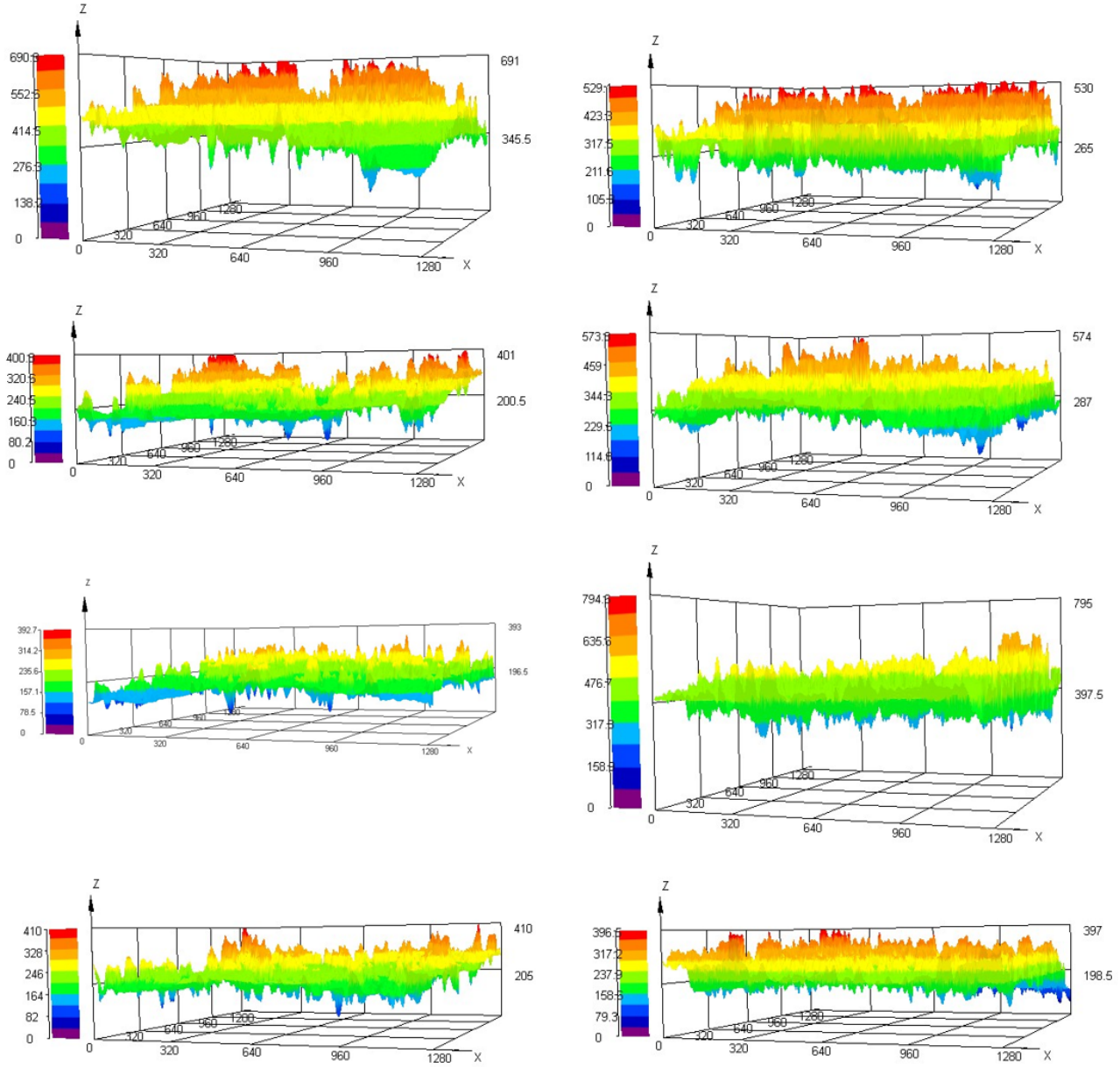

Fig. 6. 3D surfaces obtained from LP-DED of Ti6Al4V as a function of powder provider and laser power.

In addition to the mean and profilometric quantitative roughness analysis, a qualitative evaluation of the printed surfaces is also investigated. Figure 6 shows the samples' topography by color 3D graphs by which it is possible to verify the symmetry of the peaks (red) and valleys (blue) and the distribution of the pronounced peaks or valleys.

4. CONCLUSIONS

This paper determined a relationship between surface roughness (CLA, RMS, skewness, and kurtosis) generated by additive manufacturing through the LP-DED process of Ti6Al4V powders for biomedical applications and process parameters (laser power and powder provider). The following conclusions can be drawn based on the results.

- The particle size influences the surface roughness due to small particles, as observed by the Carpenter powder not governed by gravity. Inter-particle forces such as Van der walls and electrostatic forces become more important. Also, the balling phenomenon favors the size of smaller particles, adhering finer particles to the part's surface. Atomization. This research showed that the laser power and the powder morphology play an important role in the roughness of the region, improving the quality of devices for medical applications.
- The laser power also contributes to the decrease of the roughness. It is due to the laser power being directly correlated to global density energy and the powder capture efficiency. A large melt pool represents high global density energy, and consequently, a large melt pool contributes to the major high powder capture efficiency. Average roughness Sa decreased by about 42% and 23%, respectively, for Carpenter and AP&C powder providers when increasing the laser power by 15% because of the better melting process of the particles.
- Quadratic roughness Sq presented similar behavior concerning the Sa, however, with slightly higher magnitudes (+29%) due to its more sensibility to topography heights' variation.
- Statistical and profilometric skewness Ssk and kurtosis Sku parameters indicate that the printed surface can be useful to cell viability (propagation, differentiation, and adhesion) given that skewness is positive kurtosis is greater than 3 (reference value), which means there is a prevalence of sharp peaks.

5. REFERENCES

Azarniya, A., Colera, X. G., Mirzaali, M. J., Sovizi, S., Bartolomeu, F., Mare, k S. W., Wits, W. W., Yap, C. Y., Ahn, J., Miranda, G., Silva, F. S., Madaah Hosseini, H. R., Ramakrishna, S., & Zadpoor, A. A. 2019. Additive manufacturing of Ti–6Al–4V parts through laser metal deposition (LMD): Process, microstructure, and mechanical properties. *Journal of Alloys and Compounds*, Vol. *804*, p. 163–191.

Averardi, A., Cola, C., Zeltmann, S. E., & Gupta, N. 2020. Effect of particle size distribution on the packing of powder beds: A critical discussion relevant to additive manufacturing. *Materials Today Communications*, Vol. *24*, p. 100964.

Bagehorn, S., Wehr, J., & Maier, H. J. 2017. Application of mechanical surface finishing processes for roughness reduction and fatigue improvement of additively manufactured Ti-6Al-4V parts. *International Journal of Fatigue*, Vol.*102*, p.135–142.

Chan, K. S., Koike, M., Mason, R. L., & Okabe, T. 2013. Fatigue Life of Titanium Alloys Fabricated by Additive Layer Manufacturing Techniques for Dental Implants. *Metallurgical and Materials Transactions A*, Vol. *44*(2), p. 1010–1022.

Gibson, I., Rosen, D., Stucker, B., Khorasani, M. 2021. Materials for Additive Manufacturing. In: Additive Manufacturing Technologies. Springer, Cham.

Greitemeier, D., Donne, C. D., Syassen, F., Eufinger, J., & Melz, T. 2016. Effect of surface roughness on fatigue performance of additively manufactured Ti–6Al–4V. *Materials Science and Technology*, Vol. *32*(7), p. 629–634.

Gockel, J., Sheridan, L., Koerper, B., & Whip, B. 2019. The influence of additive manufacturing processing parameters on surface roughness and fatigue life. *International Journal of Fatigue*, Vol *124*, p.380–388.

Hacking, S. A., Boyraz, P., Powers, B. M., Sen-Gupta, E., Kucharski, W., Brown, C. A., & Cook, E. P. 2012. Surface roughness enhances the osseointegration of titanium headposts in non-human primates. *Journal of neuroscience methods*, vol. *211*(2), p. 237–244.

Hatamleh, M. M., Wu, X., Alnazzawi, A., Watson, J., & Watts, D. 2018. Surface characteristics and biocompatibility of cranioplasty titanium implants following different surface treatments. *Dental Materials*, Vol. *34*(4), p. 676–683.

Jemat, A., Ghazali, M. J., Razali, M., & Otsuka, Y. 2015. Surface Modifications and Their Effects on Titanium Dental Implants. *BioMed research international*, *2015*, 791725.

Krishna Alla, R., Ginjupalli, K., Upadhya, N., Shammas, M., Krishna Ravi, R., & Sekhar, R. (2011). Surface roughness of implants: A review. *Trends in Biomaterials and Artificial Organs*, *25*(3), 112-118.

Kwak, T. Y., Yang, J. Y., Heo, Y. B., Kim, S. J., Kwon, S. Y., Kim, W. J., & Lim, D. H. (2021). Additive manufacturing of a porous titanium layer structure Ti on a Co-Cr alloy for manufacturing cementless implants. *Journal of Materials Research and Technology*, Vol. *10*, p. 250-267.

Leary, M. 2017. *Surface roughness optimization for selective laser melting (SLM): Accommodating relevant and irrelevant surfaces*. In M. Brandt (Ed.), *Laser Additive Manufacturing*, Woodhead Publishing. p. 99–118.

Li, P., Warner, D. H., Fatemi, A., & Phan, N. 2016. Critical assessment of the fatigue performance of additively manufactured Ti–6Al–4V and perspective for future research. *International Journal of Fatigue*, Vol. *85*, p. 130–143.

Oyelola, O., Crawforth, P., M'Saoubi, R., & Clare, A. T. 2018. On the machinability of directed energy deposited Ti6Al4V. *Additive Manufacturing*, Vol. *19*, p. 39–50.

Selcuk C. 2011. Laser metal deposition for powder metallurgy parts, *Powder Metallurgy*, Vol. 54:2, p. 94-99,

Tolochko, N. K., Mozzharov, S. E., Yadroitsev, I. A., Laoui, T., Froyen, L., Titov, V. I., & Ignatiev, M. B. 2004. Balling processes during selective laser treatment of powders. *Rapid Prototyping Journal*, Vol. *10*(2), p. 78–87.

Sivamani, S., Nadarajan, M., Kameshwaran, R., Bhatt, C. D., Premkumar, M. T., & Hariram, V. 2020. Analysis of cross-axis wind turbine blades designed and manufactured by FDM-based additive manufacturing. *Materials Today: Proceedings*, Vol *33*, p. 3504–3509.

Yang, K. V., de Looze, G. R., Nguyen, V., & Wilson, R. S. 2022. Directed-energy deposition of Ti-6Al-4V alloy using fresh and recycled feedstock powders under a reactive atmosphere. *Additive Manufacturing*, Vol *58*, p. 103043.

Ye, C., Zhang, C., Zhao, J., & Dong, Y. 2021. Effects of Post-processing on the Surface Finish, Porosity, Residual Stresses, and Fatigue Performance of Additive Manufactured Metals: A Review. *Journal of Materials Engineering and Performance*, Vol. *30*(9), p. 6407–6425.

Svetlizky, D., Das, M., Zheng, B., Vyatskikh, A. L., Bose, S., Bandyopadhyay, A., Schoenung, J. M., Lavernia, E. J., & Eliaz, N. 2021. Directed energy deposition (DED) additive manufacturing: Physical characteristics, defects, challenges and applications. *Materials Today*, Vol. *49*, p. 271–295.

Wennerberg, A. Albrektsson, T. 2000. Suggested guidelines for the topographic evaluation of implant surfaces. *The International Journal of Oral*, Vol. *15*(3), p. 331–344.

Wong M, Eulenberger J, Schenk R, Hunziker E. 1995 Effect of surface topology on the osseointegration of implant materials in trabecular bone. J Biomed Mater Res; Vol. 29(12): p. 1567–75.

Zareidoost, A., Yousefpour, M., Ghaseme, B., & Amanzadeh, A. 2012. The relationship of surface roughness and cell response of chemical surface modification of titanium. *Journal of Materials Science: Materials in Medicine*, Vol. *23*(6), p. 1479–1488.

6. RESPONSIBILITY NOTICE

This Research was financed in part by the Coordenação de Aperfeiçoamento de Pessoal de nível Superior - CAPES - Finance code 001 and Conselho Nacional de Desenvolvimento Cientifico e Tecnológico - CNPQ.